Quantum confinement and electron spin resonance characteristics in Si-implanted silicon oxide films

V. A. Gritsenko,[1] V. A. Nadolinny,[2] K. S. Zhuravlev,[1] J. B. Xu,[3] and H. Wong[4,a)]
[1]*Institute of Semiconductor Physics, Novosibirsk, 630090, Russia*
[2]*Institute of Inorganic Chemistry, Novosibirsk, 630090, Russia*
[3]*Electronic Engineering Department, The Chinese University of Hong Kong, Shatin, Hong Kong*
[4]*Electronic Engineering Department, City University, Kowloon, Hong Kong*

(Received 15 August 2010; accepted 1 March 2011; published online 19 April 2011)

The nature of electron and hole trapping in silicon ion–implanted silicon oxide (SiO_2) with a dose of 10^{16} cm^{-2} were studied using photoluminescence and electron spin resonance (ESR) measurements. We observed an ESR signal with $g = 2.006$ after hole and electron injections. These results unambiguously imply that the Si nanoclusters created by the high-dose Si implants are both electron and hole traps in the SiO_2 films. © *2011 American Institute of Physics*.
[doi:10.1063/1.3573482]

I. INTRODUCTION

It was found that silicon nanoclusters embedded in a wide bandgap dielectric, such as amorphous silicon oxide (SiO_2) or silicon nitride (Si_3N_4), can emit strong light in the near-infrared or visible spectrum at room temperature.[1,2] A light amplification phenomenon in this material was also found.[3] The optical absorption and luminescence of Si nanoclusters/dots embedded in silicon oxide or silicon nitride were attributed to quantum confinement effects and have received widespread attention.[4–8] In addition to having an attractive luminescence property, dielectric-embedded silicon nanoclusters caught the attention of researchers working on silicon memory devices.[9–11] The nonstoichiometric Si-rich silicon nitride ($SiN_{x<4/3}$) and Si-rich silicon oxide ($SiO_{x<2}$) films demonstrate a memory effect by localizing the injected electrons or holes in deep traps with lifetimes of over ten years at room temperature.

Although a large number of experiments and theoretical studies have been conducted, the atomic and electronic structures of the deep electron and hole traps responsible for the memory effect in the oxide and nitride films are still unclear. After hole injection into the SiO_x film prepared by Si implantation into SiO_2, Kalnitsky *et al.* observed an electron spin resonance (ESR) signal related to the *E'* center.[12] Pacchioni and Ierano[13] suggested that an *E'* center can be created after hole capture in a neutral diamagnetic $O_3Si–SiO_3$ defect. In other words, after the hole capturing, a positively charged paramagnetic defect would be formed via the reaction $O_3Si–SiO_3 + h \rightarrow O_3Si{\cdot}^{+}SiO_3$. Here h represents a hole and the symbols (–) and (·) mean a normal chemical bond and an unpaired electron, respectively. This proposal was confirmed through ESR measurements. However, Afanas'ev and Stesmans found that there is no ESR signal after hole capturing in the silicon clusters of a Si-rich oxide film.[14] Therefore the nature of the electron and hole traps in Si-rich silicon oxide responding to the memory effect is still not fully understood.[15] Oxygen-deficiency defects are expected to be created in the Si-implanted SiO_2, as in the case of conventional thermal oxides.[16,17] This paper aims to provide a better understanding of the atomic and electronic structures of the oxide traps responsible for electron and hole localization in Si-rich silicon oxide using photoluminescence and ESR measurements.

II. EXPERIMENT

The oxide film used in this investigation was grown by wet thermal oxidation and was 355 nm thick (measured by ellipsometry) on a p-type ⟨111⟩ silicon wafer with a high resistivity (500 Ω·cm). Si ion implantation was done with a 50 keV ion beam and a dose of 10^{16} cm^{-2}. To remove the radiation defects in the SiO_2 film, the samples were annealed in a dry nitrogen ambient atmosphere at 800 °C for 30 min after the implantation. The implanted Si profile extends to about 120 nm and has a peak concentration of about 2×10^{21} cm^{-3} (~3%) at a distance of 60 nm below the surface. At this peak concentration, the chemical composition of the nonstoichiometric oxide is $SiO_{1.91}$.

The photoluminescence (PL) spectra of the samples in the wavelength range of 340 to 820 nm were excited using a 5 mW HeCd laser with 325 nm radiation. To measure the PL decay, a N_2 laser with a pulse width of 7 ns and a power of 10 mW was used as an excitation source. The PL signal was spectrally resolved and detected using a double diffraction grating monochromator and a cooled S-20 photomultiplier operating in the photon counting mode. The PL measurements were conducted at room temperature.

For ESR measurements, a rectangular sample with a size of $4 \times 12 \times 0.5$ mm^3 was used. The ESR measurements were conducted at room temperature using a Varian E-109 spectrometer operating in the X band with a high-frequency modulation amplitude of 0.1 G. Diphenyl-picryl-hydrazyl (DPPH) was used for the *g*-value calibration. The determination of *g*-values was made via the detection of ESR signals from both the sample and the etalon (DPPH). To maximize the signal-to-noise ratio, each spectrum was accumulated from 400 scans. Relatively high microwave power (2 mW) was used to detect

a)Electronic mail: eehwong@cityu.edu.hk.

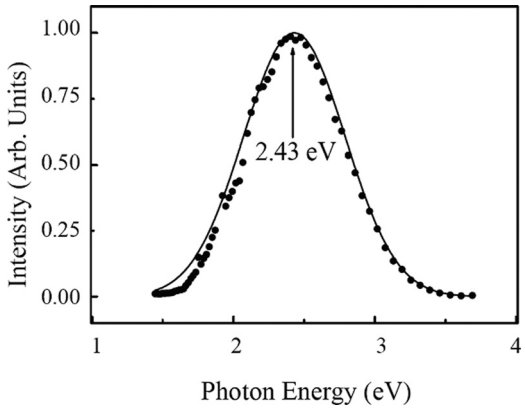

FIG. 1. Photoluminescence spectra of a Si-implanted SiO_2 film. The dots represent experimental data, and the solid line is the fitting result using the Gaussian approximation. The wavelength of the excitation source is 325 nm.

the $Si_3Si\cdot$ defects. The defect density cannot be properly determined at this power because of the saturation effect.[18] Therefore, a lower microwave power (0.2 mW) with a $CuSO_4\cdot 5H_2O$ etalon was used to measure the defect density. This low power level did not cause any saturation of the ESR signal, as confirmed by the signal level measurement on the $CuSO_4\cdot 5H_2O$ etalon sample. For electron and hole injection experiments, corona discharge plasma was used.[19] The samples used for ESR experiments were annealed in dry nitrogen at 800 °C for 30 min after implantation to remove the radiation defects in SiO_2. The same Si-implanted samples were used for the photoluminescence measurements.

III. RESULTS AND DISCUSSION

Figure 1 shows the experimental PL spectrum for the Si-implanted SiO_2 film. The PL spectrum can be approximated by a Gaussian distribution with a peak at the energy of 2.43 eV and a full width at half maximum (FWHM) of 0.84 eV. In pure SiO_2 film, there are two well-known PL peaks. The PL with the peak close to 1.9 eV originates from the nonbridging oxygen hole center (NBOHC) or onefold-coordinated oxygen atom with an unpaired electron, i.e., $\equiv$ SiO·. The second peak at 2.7 eV is due to the twofold-coordinated silicon atom with two paired electrons, i.e., = Si:.[16] However, the present sample does not show any PL peaks corresponding to these point defects. In addition, the present experimental FWHM of the PL peak is much larger than the PL peak for the sililene center (which is 0.5 eV) or that for the NBOHC (which is 0.18 eV).[16] Meanwhile, according to Anedda *et al*. and to Seol, Leki, and Onki, the PL decay times for the 1.9 eV $\equiv$ SiO· defect and the 2.7 eV = Si: center are 12 μs and 10.5 ms, respectively.[20,21]

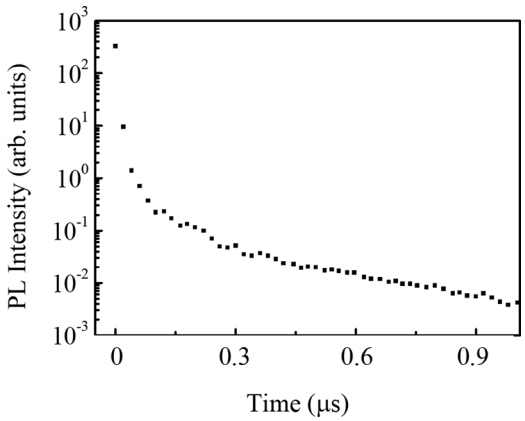

FIG. 2. Kinetic dependence of the photoluminescence intensity of Si-implanted SiO_2. A N_2 laser with a pulse length of 7 ns and a power of 10 mW was used for the decay curve measurements.

In the present study, a more reliable verification of the PL origin in the Si-implanted SiO_2 was conducted by measuring the PL decay curve, which is shown in Fig. 2. The process can be described by a sum of two exponents with decay times of about 9 ns and 0.18 μs only. These time constants are 1 to several orders of magnitude shorter than those of the NBOHC or sililene centers.[20,21] This means that the PL characteristics from Si-implanted SiO_2 are completely different from the intrinsic point defects in pure SiO_2 film. The PL in the Si-implanted sample should result from a different radiation mechanism. We suggest that the observed green PL in Si-implanted SiO_2 could be due to the quantum confinement of isolated amorphous silicon clusters in the SiO_2 matrix. The average size of the amorphous silicon clusters of the present sample can be estimated to be about 1.7 nm using the theory proposed by Park, Kim, and Park.[22]

Besides the SiO_2 matrix and the Si clusters, the sample also contains some suboxides, consisting of SiO_3Si, SiO_2Si_2, and $SiOSi_3$ tetrahedral in the Si-implanted SiO_2. The fluctuation of the SiO_x local chemical composition would result in the formation of large-scale potential fluctuation for both electrons and holes (see Fig. 3). In Fig. 3, the bandgaps for amorphous silicon and amorphous SiO_2 were taken as 1.6 eV and 8.0 eV, respectively.[23,24] The bandgap for suboxide SiO_x is in the range of 1.6 to 8.0 eV.[24] Figure 3 also depicts the proposed model for large-scale potential fluctuations caused by the variations in the local chemical composition of SiO_x which is modified based on the SiN_x model reported earlier.[27] This diagram illustrates all of the possible local (spatial) structures of the silicon oxide. The energy band diagram refers to the A-A plane; the top straight line indicates the level to which the electron energies are referred, i.e., the vacuum level. Thus, a decrease with E_g in the bandgap with E_g is evidence of the presence of SiO_x suboxides in the silicon oxide matrix. The minimum bandgap width ($E_g = 1.6$ eV) corresponds to the amorphous silicon phase. This model assumes a smooth variation of the chemical composition at the boundaries between silicon clusters in the SiO_x matrix. Our experimental data do not allow us to estimate the size of this transition region. We reckon that this size may be on the order of several dozen angstroms.

Region 1 in Fig. 3(a) corresponds to a "quantum" cluster, with dimension L on the order of the de Broglie wavelength for a quasifree electron in a silicon cluster embedded in the SiO_2 matrix. The ground state energy in this one-dimensional cluster is $E = \hbar^2/2m^*L^2$, where m^* is the effective mass of the electron. Region 2 represents a large silicon cluster surrounded by SiO_2. No energy level quantization occurs in this cluster. Region 3 is a macroscopic silicon cluster surrounded by a silicon suboxide phase. The transition

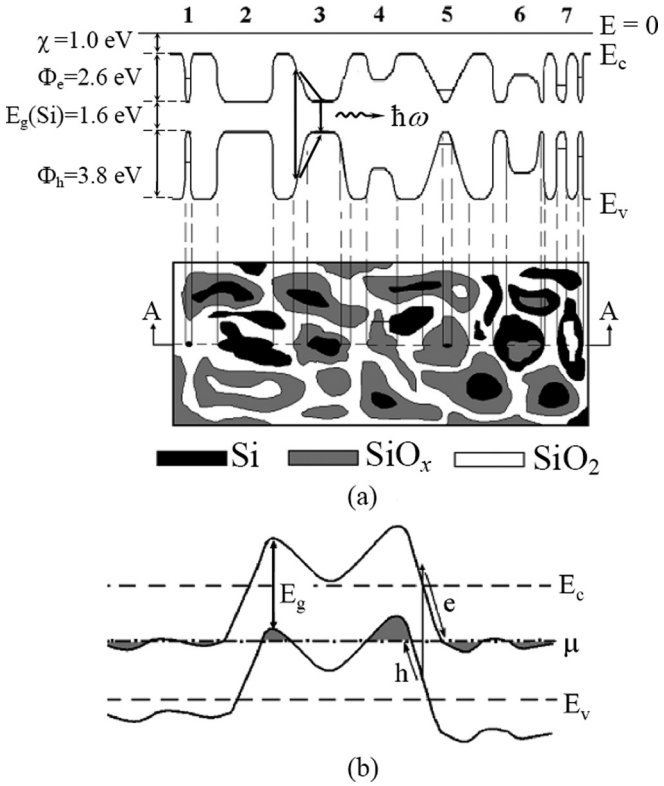

FIG. 3. Schematic diagram illustrating the proposed electronic structure of the SiO_x films. (a) Two-dimensional diagram of the SiO_x structure showing the regions of a silicon phase, the stoichiometric silicon oxide, and the suboxides (bottom) and energy band diagram of SiO_x (top) in the A-A plane as marked in the bottom diagram. E_c and E_v represent, respectively, the bottom of the conduction band and the top of the valence band; Φ_e and Φ_h are the energy barriers for electrons and holes at the a-Si/SiO_2 interfaces, respectively; E_g is the width of the bandgap; and χ is the electron affinity. (b) Illustration of the Shklovskii–Efros potential fluctuation in a heavily doped semiconductor, where μ is the Fermi level.

from silicon to SiO_2 in the energy diagram is smooth. Note that here and below, we assume that the size of the transition region occupied by silicon suboxides is significantly greater than the length of the Si–O and Si–Si bonds (amounting to a silicon suboxide cluster in the silicon oxide matrix). Region 5 is a "quantum" silicon cluster incorporated into the suboxide phase, and Regions 6 and 7 represent, respectively, the suboxide and oxide clusters, surrounded by silicon. The fluctuations of the local chemical composition of SiO_x translate into large-scale spatial fluctuations of the potential for electrons and holes. Similar models of large-scale potential fluctuations have been developed for Si:H,[26] SiC:H,[27] and SiN_x.[25] When an electron–hole pair is generated in the silicon suboxide, the electric field is directed similarly for both the electron and the hole, thus favoring their recombination [see Fig. 3(a)]. In the case of a radiative recombination mechanism, SiO_x is an effective radiative medium. Figure 3(b) illustrates the Shklovskii–Efros model of large-scale potential fluctuations in a heavily doped semiconductor.[28] According to this model, the width of the bandgap is position-invariant and the potential fluctuations are caused by the inhomogeneous spatial distribution of charged (ionized) donors and acceptors. Here, the electron–hole pair production is accompanied by a spatial separation of the electron and the hole, and thus the recombination is unfavorable.

To support the proposal of the existence of silicon clusters in the Si-implanted SiO_2, ESR experiments were conducted. As shown in Fig. 4, the virgin Si-implanted SiO_2 (trace a) has a central signal with a g-factor of 2.0062 ± 0.0006 and a linewidth of 0.65 ± 0.02 mT. This signal should be related to the radiation defects. A neutral paramagnetic threefold-coordinated silicon atom with an unpaired electron ($Si_3Si\cdot$ or D center) was identified with an ESR measurement in amorphous silicon[29] and Si:H.[30] The D center has a g-factor of 2.0055 and a linewidth of 0.47 mT. A neutral paramagnetic $Si_3Si\cdot$ defect was also observed with ESR in Si-implanted SiO_2,[31] SiO_x,[32–34] SiN_x,[35–37] SiO_xN_y films,[38,39] at the $\langle 111 \rangle$ Si/SiO_2 interface (termed a P_B center),[40] and at the Si/Si_3N_4 interface (P_N center).[41] The unpaired electron in the $Si_3Si\cdot$ defect is a hybridization of about 10% s and 90% p wavefunctions.

After being annealed in dry nitrogen at 800 °C for 30 min, the central line vanished (see trace b in Fig. 4); i.e., the radiative paramagnetic defects were removed after the annealing. Consequently, the electron and hole traps in the annealed film are diamagnetic and should not be related to the paramagnetic $\equiv Si\cdot$ defect. It is well known that the threefold-coordinated silicon atom, with an unpaired electron, $\equiv Si\cdot$, is a nonradiative recombination center in amorphous silicon, in SiO_xN_y, and at the Si/SiO_2 interface.[40,42] Therefore the absence of the $\equiv Si\cdot$ defect in Si-implanted SiO_2 after annealing can give rise to a strong luminescence with a high external quantum yield.

No ESR signal could previously be observed in the virgin silicon-rich nitride SiN_x at room temperature.[19] Even after electron or hole injection, the ESR signal was still undetectable.[19,43,44] In contrast to these experiments, in this work, the ESR signals are quite strong after electron or hole injection (see traces c and d of Fig. 4). The electron injection had resulted in the appearance of an intense ESR signal with a g-factor of 2.0062 and a linewidth of 0.65 ± 0.02 mT. For hole injection, the central ESR signal has a g-factor of

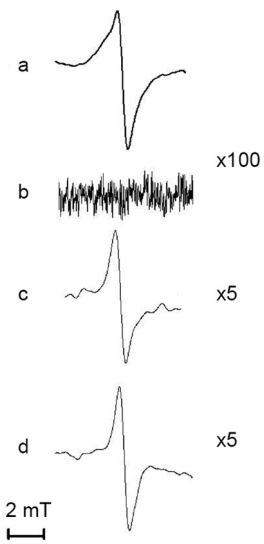

FIG. 4. Electron spin resonance signals of various samples: (a) Si-implanted SiO_2 without annealing; (b) implanted sample with annealing; (c) annealed sample with electron injection; and (d) annealed sample with hole injection.

2.0062 ± 0.0006 and a linewidth of 0.65 ± 0.02 mT. By doubly integrating the ESR signal, the surface defect density is estimated to be $(5 \pm 2) \times 10^{13}$ cm^{-2}.

Si nanoclusters were found in the Si-implanted SiO_2 by many groups.[6,18,45–47] The average size of the Si nanoclusters was estimated to be in the range of 2 to 6 nm.[6,45–47] These results support our proposed model. The existence of paramagnetic D centers after electron and hole injection into the SiO_2 films unambiguously indicates that the silicon nanoclusters in silicon oxide films are both electron and hole traps. There are two possibilities for carrier capturing in the silicon nanoclusters. The first scenario is that the carrier is localized in the bulk of the nanocluster, and the second scenario is that the localization of the carrier occurs at the silicon nanocluster/SiO_2 interface. For "bulk" localization, we can consider that the silicon nanocluster consists of $Si_3Si–SiSi_3$ species, and the hole and electron capture in the $Si_3Si–SiSi_3$ species can be described by the following equations:

$$Si_3Si - SiSi_3 + h \rightarrow Si_3Si\cdot^{+} SiSi_3, \quad (1)$$

$$Si_3Si - SiSi_3 + e \rightarrow Si_3Si^{-} : \cdot SiSi_3. \quad (2)$$

According to Eq. (1), a hole capture in a $Si_3Si–SiSi_3$ species will result in a neutral paramagnetic $Si_3Si\cdot$ defect and a positively charged diamagnetic threefold-coordinated silicon atom, $^{+}SiSi_3$. Following an electron capture on the same defect, a neutral paramagnetic defect, $\cdot SiSi_3$, and a negatively charged diamagnetic threefold-coordinated defect, Si_3Si^{-}:, will be created [see Eq. (2)].

On the other hand, if the carrier captures take place at the silicon cluster/SiO_2 interface, the Si–Si bond defect ($Si_3Si–SiO_3$) will govern the charge localization. The hole and electron capture in the Si–Si defect can be described by Eqs. (3) and (4), respectively:

$$Si_3Si - SiO_3 + h \rightarrow Si_3Si\cdot^{+} SiO_3, \quad (3)$$

$$Si_3Si - SiO_3 + e \rightarrow Si_3Si\cdot : {}^{-}SiSi_3. \quad (4)$$

A hole capture in a $Si_3Si–SiO_3$ species results in the creation of a neutral paramagnetic $Si_3Si\cdot$ defect and a positively charged diamagnetic $^{+}SiO_3$ defect, whereas an electron capture in a $Si_3Si–SiO_3$ species would produce a neutral paramagnetic $Si_3Si\cdot$ defect and a negatively charged diamagnetic:$^{-}SiO_3$ defect. This means that, in both cases, the neutral threefold paramagnetic defect $Si_3Si\cdot$ will be formed, and the occurrence of the ESR signal after electron or hole localization cannot be used to differentiate whether the carrier localization takes place in the bulk of the silicon nanocluster or at the nanocluster/SiO_2 interface.

It was found that a weak Si–Si bond in *a*–Si:H film can capture both electrons and holes with the result of a paramagnetic defect.[30] This conjecture is confirmed in the present experiment. After injecting electrons into the amorphous Si:H film, an ESR signal with $g = 2.005$, close to the value of the D center, was observed.[30] Stutzman and Biegelsen observed a hyperfine doublet splitting of 7.0 mT for D centers in Si-enriched amorphous silicon.[29] The hyperfine doublet splitting of 7.0 mT is a consequence of the hybridization of about 10% *s* and about 90% *p* unpaired electron wavefunctions. Similar to the amorphous Si:H film, the electron localization in Si-implanted SiO_2 is attributed to the creation of a $\equiv Si_3Si\cdot$ paramagnetic defect. The signal line with $g = 2.005$ observed in the sample after the electron localization suggests that the electrons were captured in the antibonding state of Si–Si or Si–O bonds. Although it was suggested that this line is related to the $HO_2Si\cdot$ defect,[37] this assignment seems untrue for the case of our samples, as the single line in the ESR spectra can be attributed to the silicon dangling bond only.

IV. CONCLUSIONS

In this work, silicon oxide embedded silicon nanoclusters were formed via the ion implantation of silicon atoms into a thick amorphous SiO_2 film. The photoluminescence experiments indicate that electron and hole quantum confinement take place in the films. The photoluminescence with a peak energy of 2.43 eV corresponds to the silicon clusters with an average size of 1.7 nm. Both electron and hole injection result in carrier capture in the silicon nanoclusters, as confirmed by electron spin resonance (ESR) measurements. The *g*-factor of the ESR spectrum unambiguously indicates that the electron and the hole should be localized in the Si atoms of the silicon nanoclusters during the carrier injection. This work reveals the nature of electron and hole traps in Si-implanted SiO_2.

ACKNOWLEDGMENTS

The work described in this paper was partially supported by the Siberian branch of the Russian Academy of Sciences (Project No. 70), a RFBR grant (Project No. 10-07-00531-a), and the Strategic Research Grant of City University of Hong Kong (Project No. 7008103). The authors would like to thank Dr. V. Filip for his help in proofreading this paper.

[1] Y. Kanemitsu and S. Okamoto, Phys. Rev. B **58**, 9652 (1998).
[2] K. Kim, Phys. Rev. B **58**, 13072 (1998).
[3] L. Pavesi, L. Dal Negro, C. Mazzoieleni, G. Franzo, and F. Priolo, Nature **408**, 440 (2000).
[4] I. Vasilev, S. Ogut, and J. Chelikowsky, Phys. Rev. Lett. **86**, 1813 (2001).
[5] N.-M. Park, C.-J. Choi, T.-Y. Seong, and S.-J. Park, Phys. Rev. Lett. **86**, 1355 (2001).
[6] F. Iacona, G. Franzo, and C. Spinella, J. Appl. Phys. **87**, 1295 (2000).
[7] C. K. Wong, H. Wong, and V. Filip, J. Nanosci. Nanotechnol. **9**, 1272 (2009).
[8] C. K. Wong, A. Misiuk, H. Wong, and A. Panas, J. Vac. Sci. Technol. B **27**, 531 (2009).
[9] V. A. Gritsenko, "Electronic structure and optical properties of silicon nitride," in *Silicon Nitride in Electronics* (Elsevier, New York 1988).
[10] E. Kameda, T. Matsuda, Y. Emura, and T. Ohzone, Solid-State Electron. **43**, 555 (1999).
[11] I. Crupi, S. Lombardo, E. Rimini, C. Gerardi, B. Fazio, and M. Melanotte, Appl. Phys. Lett. **81**, 3591 (2002).
[12] A. Kalnitsky, J. P. Ellul, E. H. Poindexter, P. J. Caplan, R. A. Lux, and A. R. Boothoroud, J. Appl. Phys. **67**, 7359 (1990).
[13] G. Pacchioni and G. Ierano, Phys. Rev. Lett. **81**, 377 (1998).
[14] V. V. Afanas'ev and A. Stesmans, Phys. Rev. B **59**, 1 (1999).
[15] J. von Borany, T. Gebel, K.-H. Stegemann, H.-J. Thees, and M. Wittmaack, Solid-State Electron. **46**, 1729 (2002).
[16] L. Skuja, J. Non-Cryst. Solids **239**, 16 (1998).
[17] W. L. Warren, E. H. Poindexter, M. Offenberg, and W. Muller-Warmuth, J. Electrochem. Soc. **139**, 872 (1992).

[18]T. Fujita, M. Fukui, S. Okada, T. Shimizu, and N. Itoh, Jpn. J. Appl. Phys. **28**, L1254 (1989).
[19]W. L. Warren, J. Kanicki, J. R. Robertson, E. H. Poindexter, and P. J. McWhorter, J. Appl. Phys. **74**, 4034 (1993).
[20]A. Anedda, G. Bongiovanni, M. Cannas, F. Congiu, and A. Mira, J. Appl. Phys. **74**, 6993 (1993).
[21]K. S. Seol, A. Leki, and Y. Ohki, J. Appl. Phys. **79**, 412 (1996).
[22]N.-M. Park, T.-S. Kim, and S.-J. Park, Appl. Phys. Lett. **78**, 2575 (2001).
[23]D. J. Lockwood, Z. H. Lu, and J.-M. Baribeau, Phys. Rev. Lett. **76**, 539 (1996).
[24]V. A. Gritsenko, *Structure and Electronic Properties of Amorphous Dielectrics in Silicon MIS Structures* (Science, Novosibirsk, Russia, 1993).
[25]A. V. Gritsenko, D. V. Gritsenko, Yu. N. Novikov, R. W. M. Kwok, and I. Bello, J. Exp. Theor. Phys. **98**, 760 (2004).
[26]W. J. Sah, H.-K. Tsai, and S.-C. Lee, Appl. Phys. Lett. **54**, 617 (1989).
[27]R. Martinos, G. Willeke, and E. Fortunato, J. Non-Cryst. Solids **114**, 486 (1989).
[28]B. I. Shklovskii and A. L. Efros, *Electronic Properties of Doped Semiconductors* (Science, Moscow, 1979).
[29]M. Stutzman and D. K. Biegelsen, Phys. Rev. B **40**, 834 (1989).
[30]T. Umeda, S. Yamasaki, J. Isoya, and K. Tanaka, Phys. Rev. B **62**, 15702 (2000).
[31]H. Hosono, H. Kawazoe, K. Oyoshi, and S. Tanaka, J. Non-Cryst. Solids **179**, 39 (1994).
[32]E. Holzenkampfer, F. W. Richter, J. Stuke, and U. Voget-Grote, J. Non-Cryst. Solids **32**, 327 (1979).
[33]Y. Kamigaki, K. Yokogawa, T. Hashimoto, and T. Uemura, J. Appl. Phys. **80**, 3430 (1996).
[34]E. San Andres, A. del Prado, I. Martil. G. Gonzalez-Diaz, D. Bravo, and F. L. Lopez, J. Appl. Phys. **92**, 1906 (2002).
[35]Y. Kamigaki, S. Minami, and H. Kato, J. Appl. Phys. **68**, 2211 (1990).
[36]S. Hasegawa, J. Appl. Phys. **83**, 2228 (1988).
[37]V. A. Gritsenko, K. S. Zhuravlev, A. D. Milov, H. Wong, R. W. M. Kwok, and J. B. Xu, Thin Solid Films **353**, 20 (1999).
[38]L.-N. He, T. Inokuma, and S. Hasegawa, Jpn. J. Appl. Phys. Part 1 **35**, 1503 (1996).
[39]B. Pivac, B. Rakvin, A. Borghesi, A. Sassella, M. Bacchetta, and L. Zanotti, J. Vac. Sci. Technol. B **17**, 44 (1999).
[40]J. F. Conley and P. M. Lenahan, in *Physics of SiO_2 and the Si/SiO_2 Interface*, edited by H. Z. Massoud, E. H. Poindexter, and C. R. Helms (Electrochemical Society, Pennington, NJ, 1996), pp. 214–249.
[41]A. Stesmans and G. Van Gorp, Phys. Rev. B **39**, 2864 (1989).
[42]H. Kato, A. Masuzawa, T. Noma, K. S. Seol, and Y. Ohki, J. Phys.: Condens. Matter **13**, 6541 (2001).
[43]V. A. Gritsenko and A. D. Milov, JETP Lett. **64**, 531 (1996).
[44]A. I. Shames, V. A. Gritsenko, R. I. Samoilova, Yu. D. Tzvetkov, L. S. Braginsky, and M. Roger, Solid State Commun. **118**, 129 (2001).
[45]P. Mutti, G. Ghislotti, S. Bertoni, L. Bonoldi, G. F. Cerefolini, L. Meda, E. Grill, and M. Gussi, Appl. Phys. Lett. **66**, 851 (1995).
[46]M. Ya. Valakh, V. A. Yukhimchuk, V. Ya. Bratis, A. A. Konchits, P. L. F. Hemment, and T. Komoda, J. Appl. Phys. **85**, 168 (1999).
[47]U. Hermann, H. H. Dunken, E. Wendler, and W. Wesch, J. Non-Cryst. Solids **204**, 273 (1996).